

Research Article

L. Borkowski*

A value of damping factor in relation to the dynamic response for a plate structure

<https://doi.org/10.2478/mme-2021-0007>

Received Aug 26, 2020; accepted Feb 25, 2021

Abstract: The subject of the research is the analysis of the impact of damping value on the dynamic response of plate. The work presents the areas of dynamic stability and instability for the different damping values and compared with the plate without damping. Furthermore, the nature of solution for each analyzed case was presented. Research by using the dynamic tools such as phase portraits, Poincaré maps, FFT analysis, the largest Lyapunov exponents were performed. The compatibility of the selected method of stability analysis with the Volmir criterion was also presented.

Keywords: Damping factor, dynamic response, phase portraits, Poincaré maps, FFT analysis, the largest Lyapunov exponents

1 Introduction

Research of plates regarding their dynamic stability began in the mid-twentieth century. The first publication about the dynamic stability of plates was Zizicas' work, which was presented in 1952[1]. In this paper, the theoretical solutions for the joint supported plate with a time-dependent load were reported. As a result of subsequent tests, criteria on the basis of which it was possible to assess dynamic stability were established. The criteria were divided into: geometric [2], energy [3] and failure [4].

An important criterion was a Budiansky-Hutchinson criterion [5], which concerned the rods and cylindrical shells with an axial load. According to their criterion, the loss of stability of dynamically loaded constructions occurs when the small load increments causes the rapid increase of deflection. A similar criterion was formulated for

cylindrical shells transversely loaded by Budiansky and Roth [6].

Another important criterion in the work of Petry and Fahlbusch was presented [4]. According to the proposed criterion, the dynamic response of the structure to the pulse load is dynamically stable if the reduced stress is smaller or equal to the ultimate stress at any time and at any point of the structure.

In 1972, Volmir proposed a criterion [7] in which the problem of dynamic stability was solved using the Bubnov-Galerkin [8] method and the resulting equations using the Runge-Kutta [9][10] method. According to the Volmir criterion, the loss of stability for the pulse load plates occurs when the maximum deflection of the plates are equal to a certain constant value – a critical value of deflection equal to the thickness or half thickness of plate is usually adopted.

The next four dynamic stability criteria were presented by Ari-Gur and Simonetta [11]. The first two criteria are based on the observation of the deflection and load pulse intensity values: if a slight increase of the load pulse intensity causes a significant increase of the value of deflection then the dynamic buckling takes place – first criterion; if a slight increase of the amplitude of the load pulse causes a decrease the value of deflection then the dynamic buckling happen – second criterion.

The third and fourth criterion is based on the response analysis of the loaded edge of plate: if a small increase of the force pulse amplitude causes a sudden increase of the shortening value of loaded edge of plate then the dynamic buckling occur – third criterion; if a small increase of the pulse intensity of displacement of loaded edge causes the change of reaction sign on the plate edge then the dynamic buckling takes place - fourth criterion.

In 1987, Kleiber, Kotula and Saran proposed the quasi-bifurcation criterion of dynamic stability based on rod systems [12]. According to this criterion, the structure loses stability and a deflection begin to grow boundlessly when the determinant of the tangent stiffness matrix is equal to zero and the absolute value of the smallest eigenvalue is greater than the absolute value of the nearest maximum, which the smallest eigenvalue reaches. In the stability the-

*Corresponding Author: L. Borkowski: Lodz University of Technology, Department of Strength of Materials, Stefanowskiego 1/15 Lodz, 90-924, Poland; Email: lukasz.borkowski@p.lodz.pl

ory of dynamical systems, a tangent stiffness matrix corresponds to the Jacobi matrix [13].

These criteria are often used by scientists dealing with dynamic stability of structures [14][15][16][17][18][19][20][21][22]. However, the analysis of plate structures applying dynamic criteria is less used [23][24][25][26][27][28]. Therefore, this paper presents the impact of damping value on the dynamic response of the plate using the dynamic tools and the compliance of the selected method of stability analysis with the Volmir criterion [7].

This article is a significant extension of the work [29], which presents the influence of damping on the dynamic response for only one value of the damping coefficient. The presented article contains several values of damping coefficients together with a complete dynamic analysis, which allows to present the nature of the solution for variable damping values. The obtained results were compared with the results for the plate without damping.

2 Studied plate

A square isotropic plate with dimensions $b=l=100\text{mm}$, $h=1\text{mm}$ (Fig. 1) was tested. The plate had the following material constants: $E=200\text{GPa}$, $\nu=0.3$. The mass of the plate is $m=78\text{g}$. The analyzed plate was simply supported on the all edges and loaded with a dynamic compressive load. The dynamic load means the load that has been introduced suddenly and lasts for an infinitely long time.

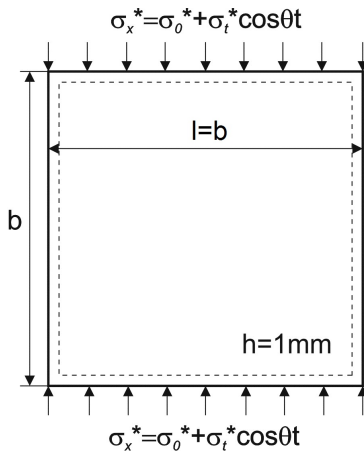


Figure 1: Studied plate.

The performed dynamic analysis of the plate structure was carried out in relation to the research presented in Volmir's work. According to the Volmir stability criterion,

the loss of stability for the pulse load plates occurs when the maximum deflection of the plates are equal to a certain constant value. Most often, the thickness or the half thickness of plate is assumed as the critical value of deflection.

2.1 The plate without damping

Using the equation presented in Volmir's work describing the plate without damping effect, we obtain:

$$\ddot{\zeta} + \omega_0^2 \left(1 - \frac{\sigma_x^*}{\sigma_{cr}^*}\right) \zeta + \eta \zeta^3 = 0 \quad (1)$$

After transforming the above equation, the equation can be written:

$$\ddot{\zeta} + \Omega_0^2 (1 - k \cos \theta t) \zeta + \eta \zeta^3 = 0 \quad (2)$$

where: $k = \frac{\sigma_t^* / \sigma_{cr}^*}{1 - \sigma_0^* / \sigma_{cr}^*}$, $\Omega_0^2 = \omega_0^2 \left(1 - \frac{\sigma_0^*}{\sigma_{cr}^*}\right)$, ζ – deflection of the plate, ω_0 – natural frequency, σ_{cr}^* – critical stress, σ_0^* – medium stress, σ_t^* – stress amplitude, η – parameter, which value is dependent on the boundary conditions.

Transforming the equation (2) to dimensionless form:

$$\ddot{x} + a(1 - k \cos \psi \tau) x + x^3 = 0 \quad (3)$$

where: $a = 1 - \frac{\sigma_0^*}{\sigma_{cr}^*}$, $\ddot{x} = \frac{\ddot{\zeta}}{\omega_0^2 \zeta_s}$, $x = \frac{\zeta}{\zeta_s}$, $x^3 = \frac{\eta \zeta^3}{\omega_0^2 \zeta_s}$, ζ_s – a static deflection, $\psi = \frac{\theta}{\omega_0}$, $\tau = \omega_0 t$ – dimensionless time. The parameters for the analyzed case are: $\omega_0=3014.3[\text{rad/s}]$, $\eta=0.23[\text{rad/mm}^2\text{s}^2]$ – the value of parameter for the plate simply supported on the all edges, $\sigma_{cr}^*=72.3[\text{MPa}]$. In order to further numerical analysis, the equation (3) has been described by two first order differential equations:

$$\begin{aligned} \dot{x}_1 &= x_2 \\ \dot{x}_2 &= -a(1 - k \cos \psi \tau) x_1 - x_1^3 \end{aligned} \quad (4)$$

2.2 The plate with damping

Modifying the equation (2) by introducing the damping effect and transforming into a dimensionless form:

$$\ddot{x} + h\dot{x} + a(1 - k \cos \psi \tau) x + x^3 = 0 \quad (5)$$

where: h – the dimensionless damping factor. For the presented research: $h=0.04; 0.02; 0.01$ [30], the other parameters are the same as for the plate without damping.

Writing the equation (5) in the form of two first-order differential equations we get:

$$\begin{aligned} \dot{x}_1 &= x_2 \\ \dot{x}_2 &= -hx_2 - a(1 - k \cos \psi \tau) x_1 - x_1^3 \end{aligned} \quad (6)$$

All studies were made for the following initial conditions: $x_1=0.01$, $x_2=0$.

3 Numerical analysis

All analyzed cases in Figs 2 and 3 using coordinates: $k - \psi/2\Omega$ ($\psi = \theta/\omega_0$, $\Omega = \Omega_0/\omega_0$) were presented. Graphs changing the values of parameters σ_0 and σ_t were created. Calculations for parameters k and $\psi/2\Omega$ changing every 0.01 were executed.

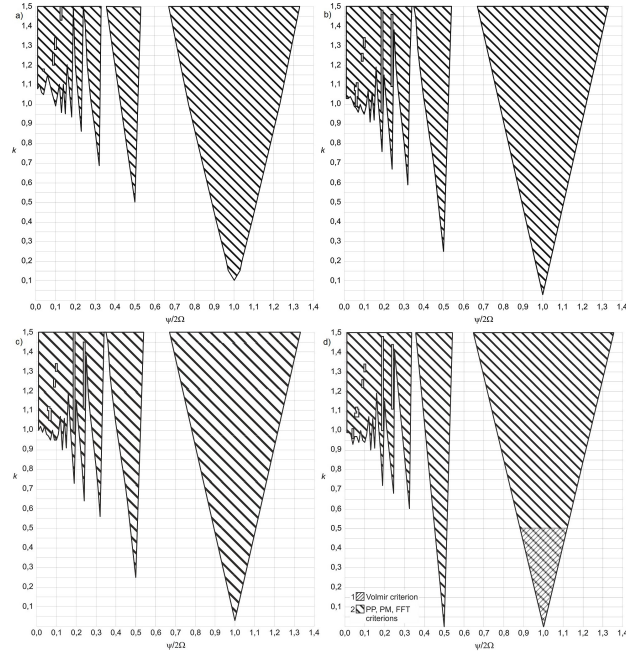


Figure 2: The graphs of dynamic stability and instability areas for the study plate with a damping factor parameter h equal to: (a) 0.04, (b) 0.02, (c) 0.01 and (d) for the plate without a damping factor.

Fig. 2 shows the areas of dynamic stability and instability (the circled areas) for the plate with a damping factor parameter h equal to: 0.04 (a), 0.02 (b), 0.01 (c) and for the plate without a damping factor (d). Fig. 2 was performed by using the criteria of phase portraits, Poincaré maps and FFT analysis.

Analyzing the areas of stability and instability (Fig. 2), it can be stated that as the damping increases, the instability areas decrease. In unstable areas there are "stability windows" in which, depending on the damping factor, appear in slightly different places

In addition, Fig. 2d contains the research presented in Volmir's work [7]. Comparing stability areas based on Volmir calculations and results obtained using dynamic tools, it can be stated that both solutions are fully compatible. The results presented in Fig. 2 are an extension of the

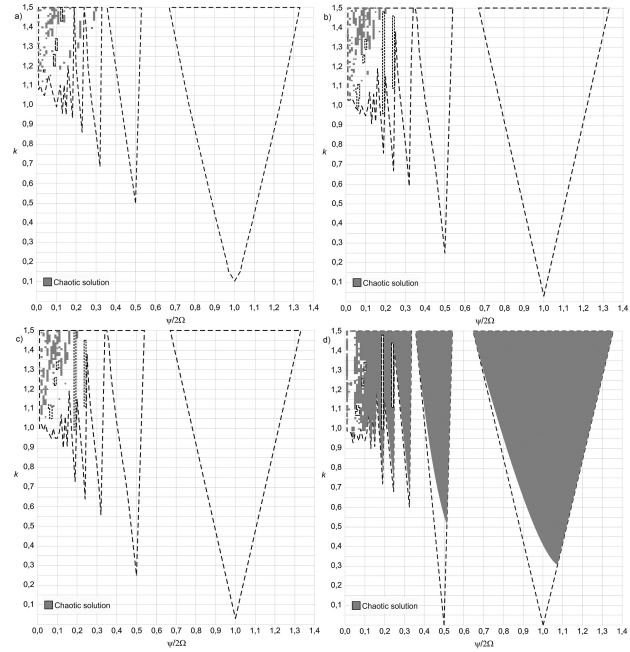


Figure 3: The graphs of areas representing the chaotic solution for the plate with a damping factor parameter h equal to: (a) 0.044, (b) 0.02, (c) 0.01 and (d) for the plate without a damping factor.

research presented by Volmir (Volmir presented areas in the field of: $k=(0.0; 0.5)$, $\psi/2\Omega=(0.85; 1.15)$).

In order to present the research results more accurately, the criterion of the largest Lyapunov exponents was used (Fig. 3). This allowed to receive information about the nature of the solution. Fig. 3 show areas of dynamic instability with a chaotic solution in gray. The dashed lines indicates the boundary for the dynamic stability/instability areas which corresponds to the circled part in Fig. 2.

Analyzing the studied plate by using the above criterion, a significant change in the solution in instability areas can be observed. For the plate with damping effect, the chaotic areas are much smaller compared to the plate without damping effect.

To more accurately present the results obtained, three points from different stability areas were selected. For the area of dynamic stability – ($k=0.50$, $\psi/2\Omega=0.70$), for the area of dynamic instability – ($k=0.40$, $\psi/2\Omega=1.00$), for the area of dynamic instability with the chaotic solution expected – ($k=1.50$, $\psi/2\Omega=0.20$). Phase portraits, Poincaré maps and FFT analysis for selected points were made (Figs 4, 5, 6).

Analyzing a selected point from the stability area (Fig. 4), it can be stated that as a result of damping the trajectory on the phase plane tends to a critical point (Fig. 4a). This is the case for all damping factor values. Consequently, the Poincaré map does not exist (Fig. 4c) and there

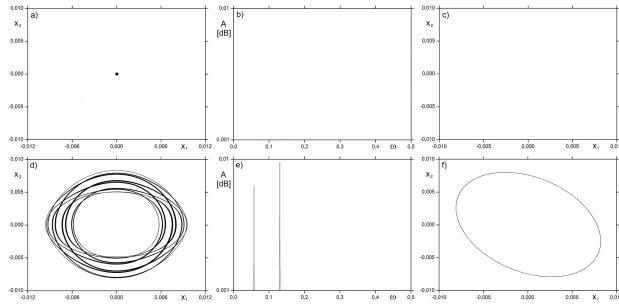


Figure 4: The point from the dynamic stability area – (a, d) phase portraits, (b, e) FFT analysis and (c, f) Poincaré maps for the plate (a, b, c) with damping factor equal 0.04, 0.02, 0.01 and (d, e, f) without damping effect.

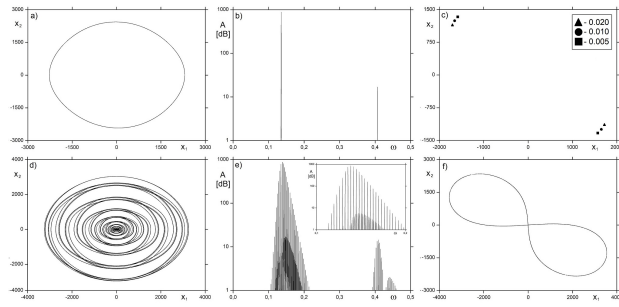


Figure 5: The point from the dynamic instability area – (a, d) phase portraits, (b, e) FFT analysis and (c, f) Poincaré maps for the plate (a, b, c) with damping factor equal 0.04, 0.02, 0.01 and (d, e, f) without damping effect.

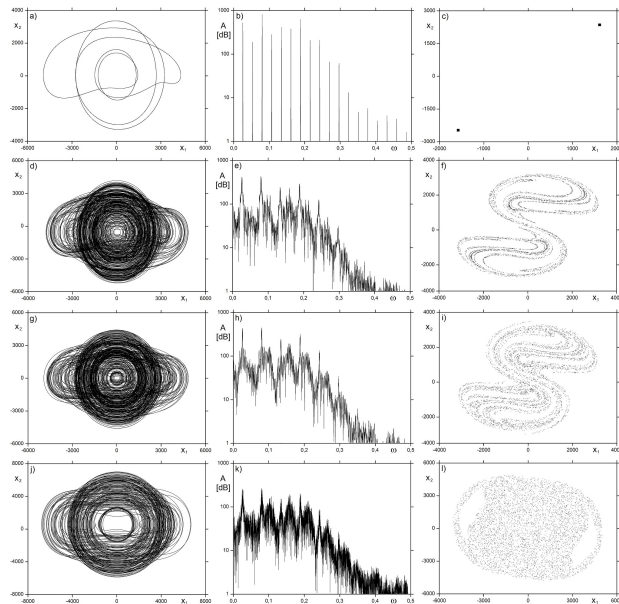


Figure 6: The point from the dynamic instability area with the chaotic solution expected – (a, d, g, j) phase portraits (b, e, h, k) FFT analysis and (c, f, i, l) Poincaré maps for the plate with damping factor equal: (a, b, c) 0.04; (d, e, f) 0.02; (g, h, i) 0.01 and (j, k, l) without damping effect.

are no dominant frequencies on the FFT analysis graph (Fig. 4b). The values of Lyapunov exponents are negative – $\lambda_1 = -0,020000$, $\lambda_2 = -0,020000$ for a damping factor of 0.04; $\lambda_1 = -0,010000$, $\lambda_2 = -0,010000$ for a damping factor of 0.02; $\lambda_1 = -0,005000$, $\lambda_2 = -0,005000$ for a damping factor of 0.01.

For the plate without damping effect a quasi-periodic solution was obtained (Figs 4d, 4f). There are two disproportionate dominant frequencies on the FFT analysis graph (Fig. 4e). There are so-called two-dimensional torus (2D torus). The values of the largest Lapunov exponents are approximately zero – $\lambda_1 = 0.000001$, $\lambda_2 = -0.000001$. It should be noted that this type of solution in the stability area is the result of the absence of damping. As a consequence, there is no attractor (attractors) to which the trajectory would converge.

Examining solutions for the instability area (Fig. 5), a significant increase in displacement x_1 and velocity x_2 in both cases can be observed – in relation to solutions from the stability area for the plate with and without damping effect (Figs 5a, 5c, 5d, 5f). For FFT analysis, there is a significant increase in signal amplitude, which was expressed in decibels (Figs 5b, 5e).

For the instability area with damping effect, a periodic solution for all three damping factors was obtained (Figs 5a, 5b, 5c). For all three damping coefficients, identical values of the dominant frequencies on the FFT analysis (Fig. 5b) and practically the same phase portrait (Fig. 5a) were observed. The values presented on the Poincaré maps differed slightly for individual values of the damping factor. On the Fig. 5c, the triangle represents the result for a damping factor of 0.04, a circle for a damping factor of 0.02, a square for a damping factor of 0.01. The differences were small enough that they were presented in one graph (Fig. 5c), similar to Figures 5a, 5b. For all three damping factors a solution with a period of 2 was reached. The FFT analysis shows one dominant frequency and its third harmonic (Fig. 5b). The values of the largest Lyapunov exponents are negative – $\lambda_1 = -0,020000$, $\lambda_2 = -0,020000$ for a damping factor of 0.04; $\lambda_1 = -0,010000$, $\lambda_2 = -0,010000$ for a damping factor of 0.02; $\lambda_1 = -0,005000$, $\lambda_2 = -0,005000$ for a damping factor of 0.01.

As in the stability area, a quasi-periodic solution for the plate without damping was acquired (Figs 5d, 5f). On the FFT analysis, two disproportionate dominant frequencies and their harmonics appear (Fig. 5e). This is a 2D torus. The values of the largest Lapunov exponents are approximately zero – ($\lambda_1 = 0.000003$, $\lambda_2 = -0.000003$).

For the last selected point with $k=1.50$, $\psi/2\Omega=0.20$ coordinates, a significant increase in displacement x_1 and velocity x_2 values compared to solutions from the stable area was also observed (Figs 6a, 6c, 6d, 6f, 6g, 6i, 6j, 6l).

The signal amplitude on the FFT analysis also increases (Figs 6b, 6e, 6h, 6k).

For the damping factor of 0.04, a periodic solution of period 2 was obtained (Figs 6a, 6b, 6c). Despite the same type of dynamic response as for the instability areas shown in Figure 5a and 5b, the analyzed area shows a more complex solution, e.g. much more harmonics appear on the FFT analysis (Fig. 6b). For this value of the damping factor, the values of Lyapunov exponents are negative – ($\lambda_1 = -0,020000$, $\lambda_2 = -0,020000$). For damping factors of 0.02 and 0.01, the selected point represents a chaotic solution (Figs 6d, 6f, 6g, 6i). On the FFT analysis, the dominant frequencies cannot be specified. The signal spectrum is continuous (Figs 6e, 6h). The values of the largest Lyapunov exponents are positive – $\lambda_1 = 0,031448$, $\lambda_2 = -0,043412$ – for the damping factor of 0.02; $\lambda_1 = 0,043478$, $\lambda_2 = -0,043478$ – for the damping factor of 0.01.

A chaotic solution for the plate without damping was also reached (Figs 6j, 6l). The FFT analysis is continuous and the dominant frequencies cannot be specified (Fig. 6k). The largest Lyapunov exponents take values: $\lambda_1 = 0,043540$, $\lambda_2 = -0,043540$.

4 Conclusions

The aim of the research was to analyze the impact of damping value on the dynamic response of plate. This paper presents stability and instability areas for various values of damping factor. They were compared with areas for a plate without damping. The assessment of the stability of the areas presented in the research and the nature of the solution was carried out using dynamic tools such as: phase portraits, Poincaré maps, FFT analysis, the largest Lyapunov exponents. The compliance of selected methods of stability analysis with the Volmir criterion was also presented.

After testing, it can be concluded that the introduction of damping to the mathematical description of the plate is of great importance in the context of dynamic response. There is a change in the occurrence of instability areas and a very big difference in solutions that are chaotic in relation to the plate without the damping effect. By changing the value of the damping factor, various solutions in instability areas were observed. As it results from the tests carried out for the last selected point ($k=1,50$, $\psi/2\Omega=0,20$), a change in the value of the damping factor affects the nature of the solution. For the damping factor equal to 0.04 a periodic solution with a period of 2, while for the remaining factors a chaotic solution was acquired.

In addition, for all analyzed points, the transition from stability to instability areas was associated with a significant increase in displacement x_1 and velocity x_2 on phase portraits and Poincaré maps. The FFT analysis showed a significant increase in signal amplitude.

Using the criterion of the largest Lyapunov exponents, negative exponents for the critical point and periodic solution were obtained. For the quasi-periodic solution the exponents had values equal to zero, and for the chaotic solution the largest exponent was positive.

For the plate with damping effect, there was a transition from a critical point to a periodic solution, and then (for damping factors equal to 0.02 and 0.01) for a chaotic solution. For the plate without damping effect, a quasi-periodic solution (2D torus), which bifurcated into a chaotic solution was presented. It should be mentioned that for all analyzed cases, the transition from periodic to chaotic solution took place through a series of period-doubling bifurcations.

Acknowledgements: This work has been supported by the Polish National Centre of Science (NCN) under project OPUS 17 nr 2019/33/B/ST8/00182.

References

- [1] Zizicas, G. A.: Dynamic buckling of thin plates, *Trans ASME*, 74(7), 1257–1268, 1952.
- [2] Cooley, J. W., Tukey, J. W.: An algorithm for the machine calculation of complex Fourier series, *Mathematics of computation*, 19(90), 297–301, 1965.
- [3] Raftoyiannis, I. G., Kounadis, A. N.: Dynamic buckling of 2-DOF systems with mode interaction under step loading, *International journal of non-linear mechanics*, 35(3), 531–542, 2000.
- [4] Petry, D., Fahlbusch, G.: Dynamic buckling of thin isotropic plates subjected to in-plane impact, *Thin-Walled Structures*, 38(3), 267–283, 2000.
- [5] Hutchinson, J. W., Budiansky, B.: Dynamic buckling estimates, *AIAA Journal*, 4(3), 525–530, 1966.
- [6] Budiansky, B., Roth, R. S.: Axisymmetric dynamic buckling of clamped shallow spherical shells, *NASA TN*, 1510, 597-606, 1962.
- [7] Volmir, A. S.: *Nonlinear Dynamics Plates and Shells*, Science, Moscow, 1972.
- [8] Michlin, S. G., Smolnicki, C. L.: *Approximate Methods for the Solution of Integral and Differential Equations*, PWN, Warsaw, 1970.
- [9] Collatz, L.: *The numerical treatment of differential equations*, Springer Science and Business Media, 2012.
- [10] Fortuna, Z., Macukow, B., Wasowski, J.: *Metody numeryczne*, WNT, Warszawa, 2002.
- [11] Ari-Gur, J., Simonetta, S. R.: Dynamic pulse buckling of rectangular composite plates, *Composites Part B: Engineering*, 28(3),

- 301–308, 1997.
- [12] **Kleiber, M., Kotula, W., Saran, M.:** Numerical analysis of dynamic quasi-bifurcation, *Engineering computations*, 4(1), 48–52, 1987.
 - [13] **Kapitaniak, T., Wojewoda, J.:** *Bifurkacje i chaos*, Wydawnictwo Naukowe PWN; Wydawnictwo Politechniki Lodzkiej, 2007.
 - [14] **Hsu, Y. C., Forman, R. G.:** Elastic-plastic analysis of an infinite sheet having a circular hole under pressure, *Journal of Applied Mechanics*, 42(2), 347–352, 1975.
 - [15] **Kowal-Michalska, K.:** About some important parameters in dynamic buckling analysis of plated structures subjected to pulse loading, *Mechanics and Mechanical Engineering*, 14(2), 269–279, 2010.
 - [16] **Kolakowski, Z., Kubiak, T.:** Interactive dynamic buckling of orthotropic thin-walled channels subjected to in-plane pulse loading, *Composite structures*, 81(2), 222–232, 2007.
 - [17] **Mania, R., Kowal-Michalska, K.:** Behaviour of composite columns of closed cross-section under in-plane compressive pulse loading, *Thin-Walled Structures*, 45(10), 902–905, 2007.
 - [18] **Kubiak, T., Kolakowski, Z., Kowal-Michalska, K., Mania, R., Swiniarski, J.:** *Dynamic response of conical and spherical shell structures subjected to blast pressure*, Proceedings of SSDS’Rio, 2010.
 - [19] **Kolakowski, Z.:** Some aspects of dynamic interactive buckling of composite columns, *Thin-Walled Structures*, 45(10), 866–871, 2007.
 - [20] **Bolotin, V.:** *Dynamic stability of elastic systems*, 1962.
 - [21] **Moorthy, J., Reddy, J. N., Plaut, R. H.:** Parametric instability of laminated composite plates with transverse shear deformation, *International Journal of Solids and Structures*, 26(7), 801–811, 1990.
 - [22] **Wu, G. Y., Shih, Y. S.:** Analysis of dynamic instability for arbitrarily laminated skew plates, *Journal of sound and vibration*, 292(1), 315–340, 2006.
 - [23] **Alijani, F., Bakhtiari-Nejad, F., Amabili, M.:** Nonlinear vibrations of FGM rectangular plates in thermal environments, *Non-linear Dynamics*, 66(3), 251–270, 2011.
 - [24] **Yuda, H., Zhiqiang, Z.:** Bifurcation and chaos of thin circular functionally graded plate in thermal environment, *Chaos, Solitons & Fractals*, 44(9), 739–750, 2011.
 - [25] **Wang, Y. G., Song, H. F., Li, D., Wang, J.:** Bifurcations and chaos in a periodic time-varying temperature-excited bimetallic shallow shell of revolution, *Archive of Applied Mechanics*, 80(7), 815–828, 2010.
 - [26] **Yeh, Y. L., Lai, H. Y.:** Chaotic and bifurcation dynamics for a simply supported rectangular plate of thermo-mechanical coupling in large deflection, *Chaos, Solitons & Fractals*, 13(7), 1493–1506, 2002.
 - [27] **Touati, D., Cederbaum, G.:** Influence of large deflections on the dynamic stability of nonlinear viscoelastic plates, *Acta mechanica*, 113(1-4), 215–231, 1995.
 - [28] **Gilat, R., Aboudi, J.:** Parametric stability of non-linearly elastic composite plates by Lyapunov exponents, *Journal of sound and vibration*, 235(4), 627–637, 2000.
 - [29] **Borkowski, L.:** Influence of the damping effect on the dynamic response of a plate, *Journal of Theoretical and Applied Mechanics*, 51(1), 263–272, 2019.
 - [30] **Kolakowski, Z., Teter, A.:** Influence of Inherent Material Damping on the Dynamic Buckling of Composite Columns with Open Cross - Sections, *Mechanics and Mechanical Engineering*, 17(1), 59–69, 2013.